

Locked Plating of Distal Femur Fractures Leads to Inconsistent and Asymmetric Callus Formation

Trevor J. Lujan, PhD,* Chris E. Henderson, MD,† Steven M. Madey, MD,* Dan C. Fitzpatrick, MD,‡
J. Lawrence Marsh, MD,† and Michael Bottlang, PhD*

Objectives: Locked plating constructs may be too stiff to reliably promote secondary bone healing. This study used a novel imaging technique to quantify periosteal callus formation of distal femur fractures stabilized with locking plates. It investigated the effects of cortex-to-plate distance, bridging span, and implant material on periosteal callus formation.

Design: Retrospective cohort study.

Setting: One Level I and one Level II trauma center.

Patients: Sixty-four consecutive patients with distal femur fractures (AO types 32A, 33A–C) stabilized with periarticular locking plates.

Intervention: Osteosynthesis using indirect reduction and bridge plating with periarticular locking plates.

Main Outcome Measurement: Periosteal callus size on lateral and anteroposterior radiographs.

Results: Callus size varied from 0 to 650 mm². Deficient callus (20 mm² or less) formed in 52%, 47%, and 37% of fractures at 6, 12, and 24 weeks postsurgery, respectively. Callus formation was asymmetric, whereby the medial cortex had on average 64% more callus ($P = 0.001$) than the anterior or posterior cortices. A longer bridge span correlated minimally with an increased callus size at Week 6 ($P = 0.02$), but no correlation was found at Weeks 12 and 24 postsurgery. Compared with stainless steel plates, titanium plates had 76%, 71%, and 56% more callus at Week 6 ($P = 0.04$), Week 12 ($P = 0.03$), and Week 24 ($P = 0.09$), respectively.

Conclusions: Stabilization of distal femur fractures with periarticular locking plates can cause inconsistent and asymmetric formation of periosteal callus. A larger bridge span only minimally improves callus formation. The more flexible titanium plates enhanced callus formation compared with stainless steel plates.

Key Words: locked plating, femur, fracture, callus, secondary bone healing, periarticular plating

(*J Orthop Trauma* 2010;24:156–162)

INTRODUCTION

The introduction of locking plates with fixed-angle screws has improved the fixation strength of plate constructs and they are frequently indicated for bridge plating of comminuted fractures.^{1–3} For supracondylar femur fractures, periarticular locking plates have been rapidly adopted as an alternative to intramedullary nails, blade plates, and non-locking condylar screws.⁴ In addition to providing fixed-angle stabilization in the osteoporotic metaphysis, these locking constructs enable biologic fixation techniques that emphasize preservation of blood supply and functional reduction over anatomic reduction and interfragmentary compression of metaphyseal fractures.⁵

Because interfragmentary compression is not obtained when these locking plates are used to bridge comminuted distal femur fractures, healing between fragments must occur by secondary bone healing with callus formation.⁶ Secondary bone healing is mediated by interfragmentary motion in the millimeter range^{7–10} and can even be enhanced by active^{7,11,12} or passive dynamization.¹³ However, locked plating constructs can be as stiff as conventional plating constructs¹⁴ designed to induce primary bone healing, which requires interfragmentary motion to remain below 0.15 mm.⁵ The relatively high stiffness of locked bridge plating constructs may therefore suppress interfragmentary motion preventing secondary bone healing.^{4,6,15} This theoretical concern is supported by recent case studies on locked plating that describe deficient callus formation,¹⁶ delayed union, late implant failure, and nonunions.^{3,17,18}

The stiffness of locked plating constructs can be decreased, to some extent, by increasing the bridging span of the plate over the fracture zone.^{19,20} Stoffel et al recommended omitting one to two screw holes on each side of the fracture to initiate spontaneous fracture healing by callus formation.²¹ The stiffness of locked plating constructs may also be decreased by plates made of flexible titanium alloy rather than stainless steel. Both of these strategies rely on elastic plate bending to increase interfragmentary motion. For a lateral distal femur plate, plate bending induces more

Accepted for publication August 27, 2009.

From the *Biomechanics Laboratory, Legacy Research & Technology Center, Portland, OR; †University of Iowa Hospitals and Clinics, Iowa City, IA; and ‡Slocum Center for Orthopedics, Eugene, OR.

Financial support for this research was provided by National Institutes of Health/National Institute of Arthritis and Musculoskeletal and Skin Diseases Grant R21 AR05361.

Reprints: Michael Bottlang, PhD, Legacy Biomechanics Laboratory, 1225 NE 2nd Avenue, Portland, OR 97215 (e-mail: mbottlan@lhs.org).

Copyright © 2010 by Lippincott Williams & Wilkins

interfragmentary motion at the medial cortex than at the lateral cortex adjacent to the plate. It therefore may result in asymmetric callus formation with the largest periosteal callus being expected at the medial cortex.

Because periosteal callus formation is the principal hallmark of secondary bone healing, we conducted a retrospective cohort study to quantify, for the first time, periosteal callus formation of supracondylar femur fractures stabilized with periarticular locking plates. The purpose was to assess the effect of construct stiffness and interfragmentary motion on callus production during the first 6 months after fracture. Three specific hypotheses were tested: 1) more callus forms at the medial cortex where plate bending induces more interfragmentary motion compared with the anterior and posterior cortices; 2) longer bridging spans lead to more callus formation than short bridging spans; and 3) titanium plates lead to more callus formation than stainless steel plates.

METHODS

This retrospective cohort study quantified periosteal callus formation of 66 distal femur fractures stabilized with periarticular locking plates. Callus size and radiodensity were extracted from lateral and anteroposterior radiographs obtained at 6, 12, and 24 weeks postsurgery. Projections of the medial, anterior, and posterior callus were evaluated separately to determine if callus formed evenly around the fracture. Furthermore, callus measurements were stratified to determine the effect of bridging span and implant material on callus formation.

Patients

A consecutive cohort of patients with distal femur fractures treated with periarticular locking plates between June 2002 and December 2007 were investigated from the University of Iowa Hospital and Clinics and the Slocum Center for Orthopaedics. The studies were approved by the Institutional Review Board of each center. Inclusion criteria were the availability of lateral and anteroposterior radiographs obtained postoperatively and at two or more follow-up times of

6, 12, and 24 weeks. To curtail artifacts from out-of-plane rotation,^{22,23} follow-up radiographs were excluded if they demonstrated a rotational deviation greater than 30° relative to the corresponding postoperative radiograph. Out-of-plane rotation was approximated by comparing screw dimensions in sequential radiographs. Revision surgeries were also excluded to eliminate confounding factors secondary to bone grafting or implant alterations. After review of 104 patients, inclusion criteria were met by 64 patients (59 ± 20 years of age, 68% female) with 66 distal femur fractures. Using the Orthopaedic Trauma Association classification,²⁴ there were three 32A fractures, 35 33A fractures, two 33B fractures, and 26 33C fractures. Thirty-five fractures were comminuted, 15 fractures were open, and 12 fractures were periprosthetic. The average follow-up time of paired anteroposterior and lateral radiographs was 6.4 ± 1.8 weeks (n = 59), 12.9 ± 2.5 weeks (n = 63), and 25.6 ± 5.7 weeks (n = 55), respectively. Fractures were treated with four different periarticular locking plates. Thirty fractures were treated with the titanium Less Invasive Stabilization System (Synthes, Paoli, PA), three fractures were treated with the titanium Polyaxial Distal Femur Plate (DePuy, Warsaw, IN), 17 fractures were treated with stainless steel Locking Compression Plates (LCP; Synthes), and 16 fractures were treated with the stainless steel PERI-LOC distal femur plate (Smith and Nephew, Memphis, TN).

Callus Extraction

Custom software was developed to objectively extract the size and radiodensity of periosteal callus from plain radiographs without the need for manual tracing of boundaries. All radiographs were transferred to digital format for image processing with MathLab software (MathWorks, Natick, MA). A region of interest was selected on each radiograph, encompassing the fractured cortex and the adjacent periosteal callus region of interest. The software first detected and outlined the cortex above and below the fracture using intensity gradients along lines nominally perpendicular to the cortex (Fig. 1A). After the proximal and distal cortices were defined, the fracture was bridged by

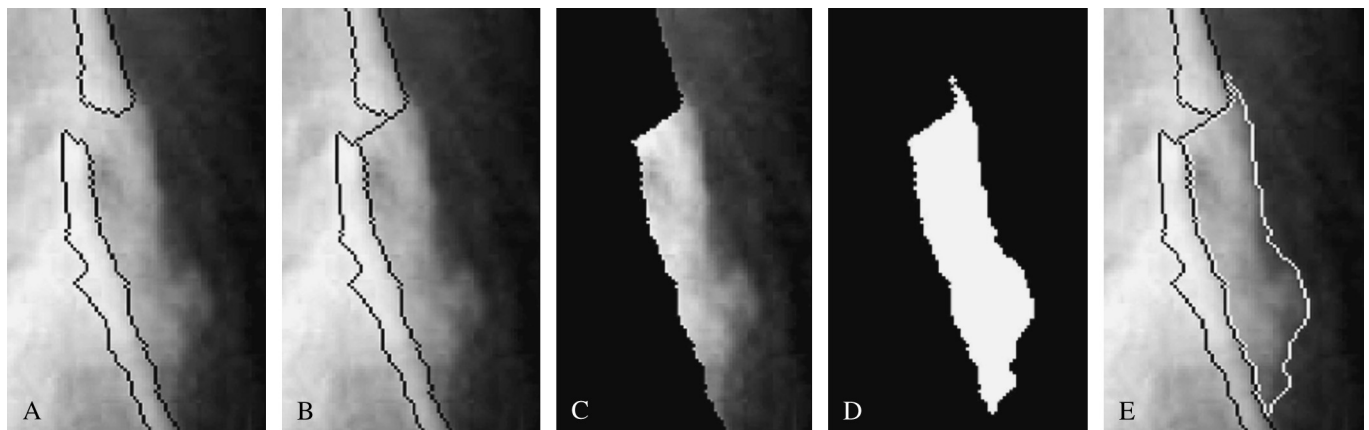


FIGURE 1. Process of defining periosteal callus. (A) Detection of cortices. (B) Connecting cortices at the fracture site. (C) Void cortices. (D) Callus segmentation by selection of pixels two standard deviations above local background intensity. (E) Demarcation of periosteal callus.

the shortest line connecting the tip of the outermost cortex with the periosteal surface of the adjacent cortex (Fig. 1B). The cortices and the intramedullary canal up to the bridging line were voided to isolate the periosteal space (Fig. 1C). Pixels were then assigned as callus based on an empiric threshold of two standard deviations²⁵ above the local background intensity (Fig. 1D). Finally, the cortex and periosteal callus boundaries were projected over the original x-ray for visual inspection (Fig 1E).

Callus Evaluation

Once the callus was outlined, callus size, radiodensity, and symmetry were evaluated. To calculate callus size, the number of pixels contained in the callus region was converted into metric area using a length standard based off implant features of known dimension. On anteroposterior radiographs, the length standard was calculated by the number of pixels spanning the known diameter of a screw. On lateral radiographs, the length standard was calculated by the number of pixels spanning the known distance between vacant screw holes. To account for bone fragments that could affect periosteal callus assessment, the area of any fragments in the periosteal space that were present on postoperative radiographs was subtracted from the callus area at each subsequent evaluation time.

The radiodensity of periosteal callus was assessed relative to the radiodensity of the cortex. A normalized callus radiodensity of 100% would therefore have the same radiodensity as the cortex. This normalized value was determined by dividing the average radiodensity of the periosteal callus area by the average radiodensity of the adjacent cortices.²⁶ Fracture regions with a callus smaller than 1 mm² were excluded from radiodensity assessment.

Verification and Validation of Callus Measurement

A rigorous verification study was conducted to quantify the algorithm's ability to measure callus size.²⁷ In brief, the numeric accuracy of the algorithm was assessed by analyzing test patterns of known dimensions. The algorithm has a numeric error less than 1% when measuring objects greater than 10 mm²; however, this error increases to 30% when measuring objects that are 1 mm². To assess error in measuring the area profile of callus, radiographs were taken of three-dimensional callus surrogates of known dimensions. The algorithm was able to measure high- and low-density callus surrogates with an error of less than 4%. To test observer variance, 10 clinical radiographs were analyzed independently by three operators. The intra- and interobserver error of this algorithm was found to be 3% and 4%, respectively.

An abridged validation protocol was implemented for clinical oversight of the algorithm results. Three clinicians independently inspected the demarcation of cortical bone and periosteal callus in every analyzed image as shown in Figure 1E. Three clinicians were deemed adequate based on a previous article that developed and validated an objective method to score fracture severity.²⁸ Two of the clinicians (DCF, SMM) were orthopaedic surgeons specializing in trauma, and one was an orthopaedic resident (CEH). Clinicians were

instructed to either accept or reject the callus boundary assigned by the algorithm (Fig. 1E, white line). Images were included in the evaluation if at least two clinicians agreed that the fracture callus had been appropriately demarcated. Of the 587 images, 565 images were accepted by all three clinicians, 19 images were accepted by only two clinicians, and three images were discarded from further evaluation as a result of lack of consensus.

Callus Symmetry

Callus symmetry was evaluated to investigate the effect of plate proximity on callus formation. The average size and radiodensity of the medial periosteal callus (MEDIAL group) was compared with the average size and radiodensity of anterior and posterior periosteal callus (A-P group). MEDIAL group callus was located at approximately twice the distance from the plate compared with callus in the A-P group. In the MEDIAL group, each of the evaluated fractures yielded a valid medial callus result at all time points. As a result of obstruction by the plate in the A-P group, only 27 anterior callus sites and 59 posterior callus sites could be evaluated with follow-up radiographs. Combining the anterior and posterior callus sites in the A-P group yielded a comparable sample number in the A-P group (n = 86) and the MEDIAL group (n = 78). There was no significant difference between the A-P and MEDIAL groups with respect to patient age ($P = 0.81$), Orthopaedic Trauma Association classification ($P = 0.92$), periprosthetic fracture ($P = 0.73$), open fracture ($P = 0.48$), implant type ($P = 0.63$), or bridging span ($P = 0.80$).

Effect of Bridge Span

To determine if a longer bridging span with apparently lower construct stiffness would improve callus formation, the bridge span over each fracture was measured in terms of the distance between the screws adjacent to the fracture. Subsequently, the bridge span was correlated to callus size.

Effect of Implant Material

To determine if more callus is formed with titanium alloy plates that are more elastic than stainless steel plates, callus measurements were stratified by implant material.

Statistical Analysis

The effect of location, implant material, and evaluation time on callus formation (size and radiodensity) was determined with analysis of variance. When significance was detected, unpaired t tests were performed between different factor levels with multiple comparisons being accounted for by adjusting P values with the Holm-Bonferroni method.²⁹ Confidence intervals were used for equivalence testing. Differences in age, fracture type, implants, and bridging span between the MEDIAL and A-P groups were analyzed with Pearson χ^2 tests. The relationship of callus size with bridge span was evaluated with Pearson r correlation coefficients, regression lines, and P values. All results are reported by their average value and standard deviation. For all statistical analyses, the significance level was set at 0.05.

RESULTS

The periosteal callus size varied greatly between patients, ranging from 0 to 670 mm². Examples of fractures without callus, with a small callus (51 mm²) and with a completely bridged callus (247 mm²) are depicted in Figure 2 for the medial cortex at 24 weeks. Overall, the average callus size at Weeks 6, 12, and 24 was 62 ± 89 mm², 93 ± 125 mm², and 114 ± 162 mm², respectively.

A considerable number of fractures formed no or very little callus. Ranking periosteal callus by size in increments of 20 mm² demonstrated that 37% of all callus measurements fell within the smallest callus size increment of 0 to 20 mm² at Week 24 (Fig. 3A). Callus measurements of greater than 20 mm² were obtained in 48%, 53%, and 63% of all cases at 6, 12, and 24 weeks postsurgery, respectively (Fig. 3B).

Callus formation was asymmetric. Compared with the A-P group, the MEDIAL group had 75% more callus at Week 6 (*P* = 0.04), 81% more callus at Week 12 (*P* = 0.02), and 39% more callus at Week 24 (*P* = 0.20, 95% confidence that difference in callus size is less than 60%) (Fig. 4). Compared with the MEDIAL group, the A-P group had a 76%, 65%, and 26% higher incidence of deficient callus formation (callus area 20 mm² or less) at Week 6 (*P* = 0.002), Week 12, (*P* = 0.001), and Week 24 (*P* = 0.10), respectively. Callus radiodensity was on average 9% greater in the MEDIAL group (60% ± 19%) than in the A-P group (55% ± 16%, *P* = 0.02).

Compared with fractures treated with stainless steel plates, fractures treated with titanium plates had 76% more

callus at Week 6 (*P* = 0.04), 71% more callus at Week 12 (*P* = 0.03), and 56% more callus at Week 24 (*P* = 0.09, 95% confidence that difference in callus size is less than 64%) (Fig. 5). At Week 24, fractures treated with titanium and stainless steel plates had deficient callus formation (callus area 20 mm² or less) in 26% and 49% of all callus sites (*P* = 0.01), respectively.

Plate constructs had on average a bridge span of 71 ± 32 mm (range, 20–157 mm). A longer bridging span correlated with a greater callus size only at Week 6 in the MEDIAL group (Fig. 6), although the correlation was weak (*r* = 0.30, *P* = 0.02). There was no significant correlation between bridging span and callus size at Weeks 12 and 24 in either the MEDIAL or the A-P group.

DISCUSSION

The inconsistent and asymmetric callus formation found in this study lends further support to the anecdotal concern that locked bridge plating constructs may be too stiff to optimally promote secondary bone healing.^{4,15} Although the majority of fractures formed sufficient periosteal callus and progressed to complete bony bridging, this study found that almost 40% of fractures developed little to no callus (20 mm² or less) even 6 months after surgery. For comparison, an area of 20 mm² is comparative to the size of a 5-mm diameter screw hole. This rate of deficient callus formation is greater than the clinically reported nonunion rate for locked plating of distal femur

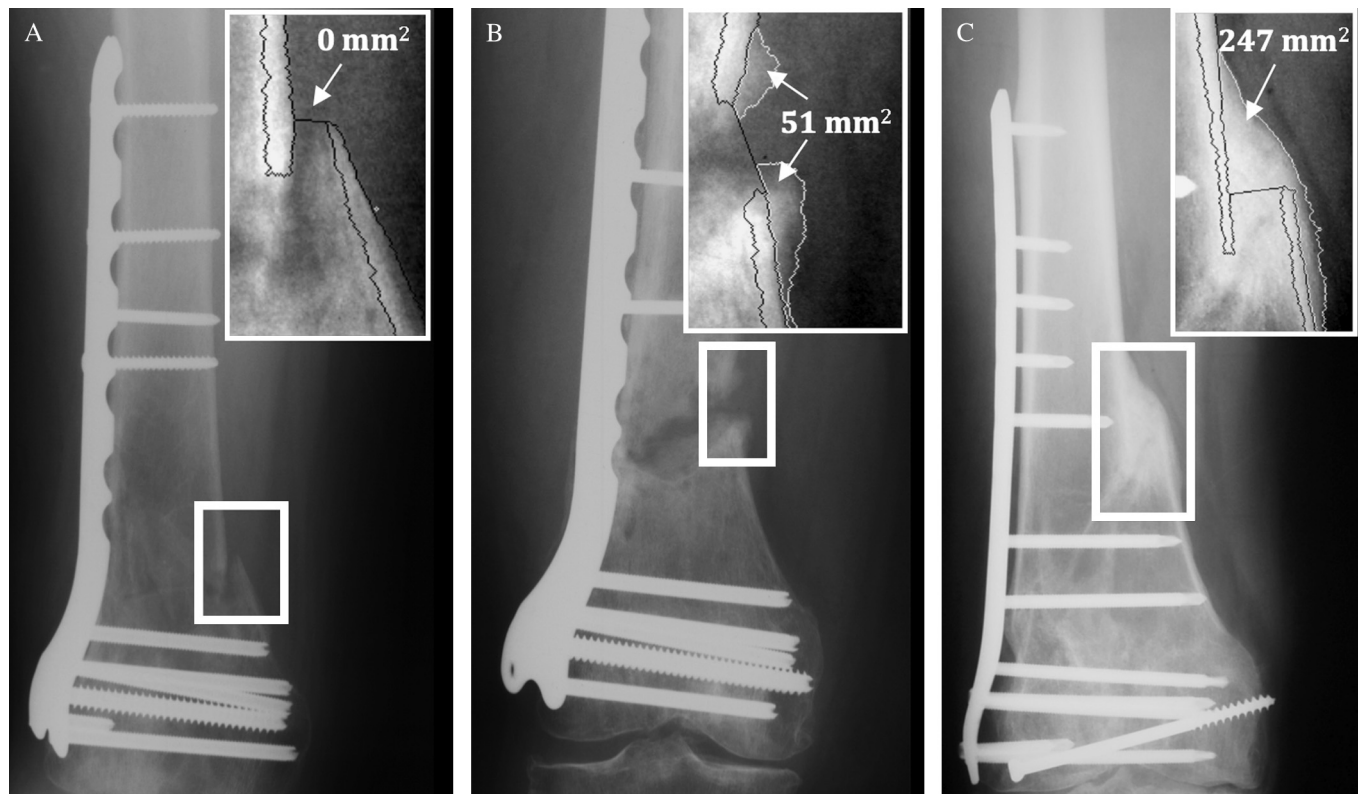


FIGURE 2. Periosteal callus measurement in three patients at Week 24. (A) No periosteal callus. (B) Small periosteal callus (51 mm²) with a normalized radiodensity of 60%. (C) Bridging callus (247 mm²) with a normalized radiodensity of 80%.

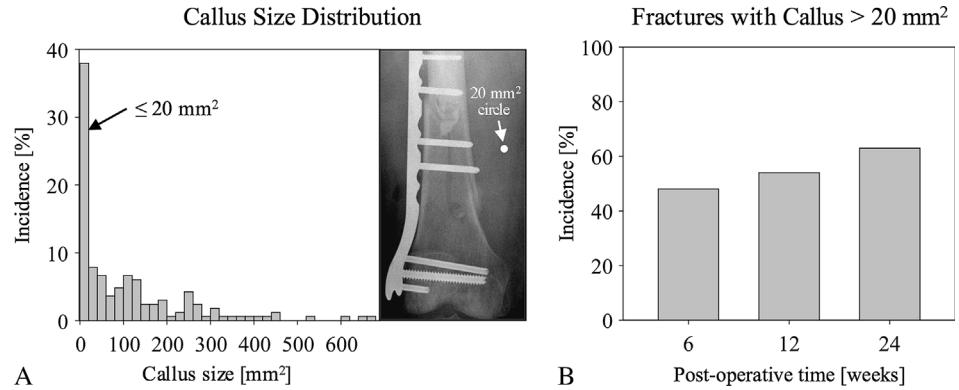


FIGURE 3. Periosteal callus distribution: (A) At 24 weeks postsurgery, 37% of all fractures had no or very little callus (20 mm² or less). (B) Percentage of fractures with callus size greater than 20 mm² at each evaluation time point.

fractures. Several small case series encompassing 13 to 25 patients reported a 100% union rate.³⁰⁻³² Other studies report nonunion rates ranging from 3%³³ to 14%³⁴ and hardware and fixation failure rates of 6%³⁵ to 20%.^{33,34} A recent systematic review of 29 case series with a total of 415 distal femur fractures found a 3.5-fold increase of nonunions associated with locked plates (5.3%) as compared with intramedullary nailing (1.5%).³⁶ In a prospective study on 54 fractures with 1-year follow up, Schutz reported 3.8% nonunions, 6% delayed unions, and 12% of patients required a secondary procedure with bone grafting.³⁷ The majority of hardware and fixation failures occurred late, after 6 months, indicating that the superior durability of locked plating constructs may conceal nonunions for a prolonged time.

Periosteal callus formation is a clinical indicator of fracture healing that correlates with mechanical rigidity at the fracture site.^{26,38,39} For example, callus formation has a high correlation to bending stiffness ($r = 0.89$)²⁶ and torsional rigidity ($r = 0.94$)³⁹ in canine tibial osteotomies. In human tibial fractures, callus formation was also predictive of bending stiffness, although the correlation was low to moderate ($r = 0.49$).³⁸ Bear in mind that an absence of periosteal callus may

not necessarily indicate a nonunion, because secondary fracture healing may in some cases occur by endosteal or intramedullary pathways.⁴⁰⁻⁴² Conversely, periosteal callus formation per se may not necessarily indicate that the plating construct permitted sufficient interfragmentary motion, because progressive loss of fixation can lead to callus formation. This has recently been described by comparison of two similar cases of periprosthetic supracondylar femur fractures stabilized with periarticular locking plates.¹⁶ One case retained stable fixation and developed a nonunion in the absence of callus formation. The other case healed by ample callus formation subsequent to loss of distal fixation, which in turn allowed for sufficient interfragmentary motion.

Asymmetric callus formation reported in the present study provides further evidence that callus stimulation is attenuated by decreasing amounts of interfragmentary motion in proximity to the plate. It reflected the asymmetric gap closure characteristic for bridge plating constructs, whereby the least amount of callus formation is to be expected at the cortex adjacent to the plate. However, deficient callus formation at the plate side is difficult to detect on planar radiographs because the plate obscures visibility. In contrast,

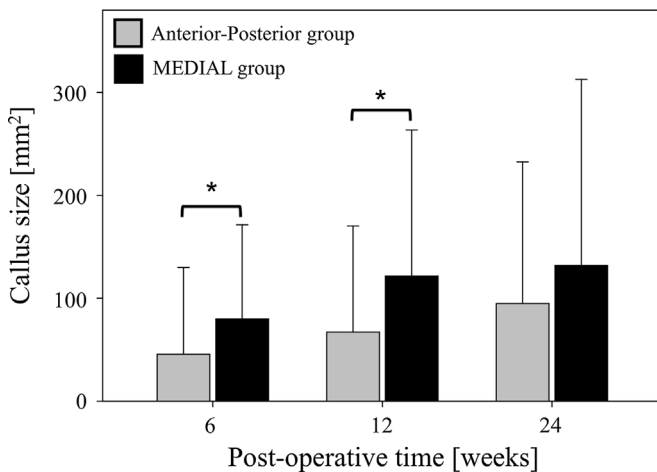


FIGURE 4. Callus formation was asymmetric with more callus being formed on the medial aspect than on the anterior and posterior aspect. * $P < 0.05$.

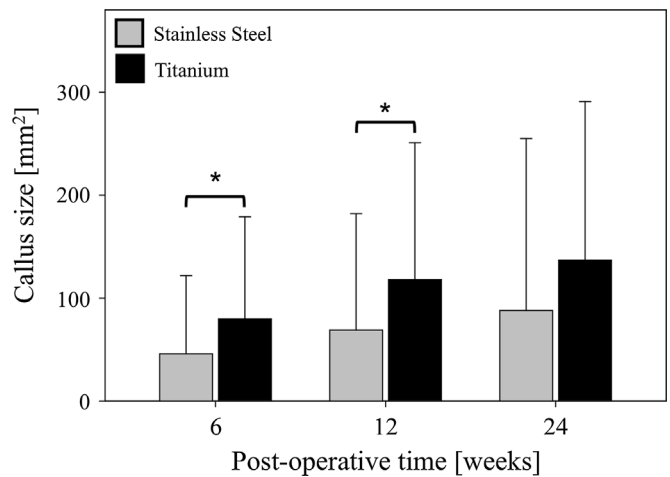


FIGURE 5. Fractures treated with titanium plates had significantly more periosteal callus at Weeks 6 and 12 than those treated with stainless steel plates. * $P < 0.05$.

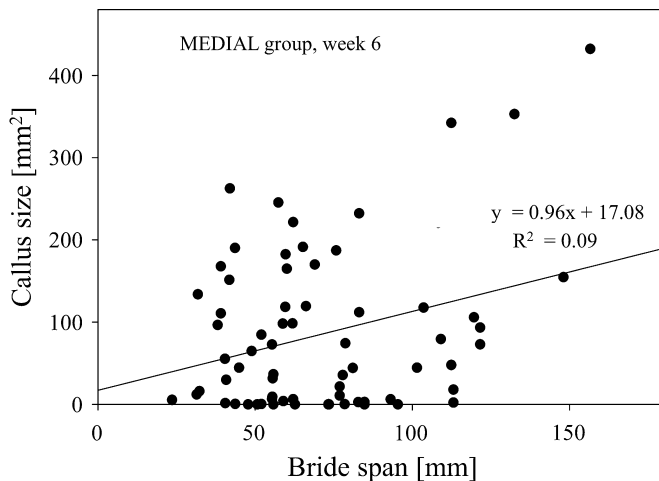


FIGURE 6. A longer bridge span correlated weakly with an increased callus size in the MEDIAL group at Week 6 ($P = 0.02$) but no correlation existed at Weeks 12 and 24 in either the MEDIAL or the A-P group.

regular callus formation around the entire cortical circumference had been reported for diaphyseal fractures treated with casts,⁴³ circular fixators,⁴⁴ and intramedullary nails.⁴⁵

Increasing the bridging span by omitting screw holes adjacent to the fracture zone has been recommended for reduction of construct stiffness to initiate spontaneous fracture healing by callus formation.¹⁹ However, the reported efficacy in stiffness reduction is inconsistent. Stoffel et al reported that increasing the plate span by omitting one screw hole on either side of the fracture made a locked plating construct (4.5-mm titanium LCP; Synthes) almost twice as flexible in both compression and torsion.¹⁹ In contrast, Fields et al reported that omitting two screws above and below the fracture had no significant effect on either bending or torsional stiffness of a conventional plate construct (4.5-mm DCP; Synthes) in a comparable bridge plating configuration.²⁰ The present study found a low correlation between increased bridge span and increased callus formation at only one time point. This result suggests that increasing the bridge span might not be sufficient to reliably promote callus formation with contemporary locked plating constructs.

Titanium implants are nominally twice as flexible as similar-sized stainless steel implants. The higher flexibility directly translates into higher interfragmentary motion, which likely was responsible for the significantly increased callus formation seen with titanium implants. Nevertheless, 26% of fracture sites stabilized with titanium plates had deficient callus formation at Week 24. This finding suggests that a further reduction in stiffness may be beneficial to decrease the incidence of deficient callus formation.

This study had several limitations. The retrospective nature of this research precluded measuring the bone mineral density of the callus, which is a strong indicator of fracture healing.⁴⁴ However, the radiodensity measurements reported in this study also serve as a good indicator of callus mineralization and bending stiffness.²⁶ The correlation between

radiodensity and stiffness is nonlinear, whereby small changes in the radiodensity of mature callus equate to larger changes in bending stiffness.²⁶ Measuring callus formation from plain radiographs only estimates what is a three-dimensional biologic process. Nevertheless, using two-dimensional radiographic projections can effectively approximate callus growth.⁴⁴ Callus formation was quantified with custom image analysis software to objectify a normally categorical and subjective process.^{46,47} Rotations of the radiograph will affect the sequential quantification of callus formation; therefore, it was necessary to exclude cases exhibiting large rotations between evaluation times. To avoid these limitations and to further investigate the asymmetric callus formation, future studies should prospectively evaluate locked bridge plating constructs using computed tomography for three-dimensional assessment of callus formation. Finally, this early time-point study only focused on radiographic evaluation of callus size. Given a longer study period that follows all patients to healing, a future study should correlate callus formation with fracture healing.

In conclusion, this study demonstrated that stabilization of distal femur fractures with locking plates can cause inconsistent and asymmetric formation of periosteal callus, which may be attributed to the high stiffness of the fixation construct. The asymmetric callus formation provided further evidence that callus stimulation is attenuated by decreasing amounts of interfragmentary motion at the cortex nearest to the plate. A larger bridge span yielded only mildly improved callus formation. The more flexible titanium plates enhanced callus formation compared with stainless steel plates. A future prospective study should use three-dimensional assessment of callus formation to further investigate deficient callus formation near the plate, where interfragmentary motion is minimal.

REFERENCES

- Kolodziej P, Lee FS, Patel A, et al. Biomechanical evaluation of the Schuhl nut. *Clin Orthop Relat Res.* 1998;347:79–85.
- Ramotowski W, Granowski R. Zespol. An original method of stable osteosynthesis. *Clin Orthop Relat Res.* 1991;272:67–75.
- Ring D, Kloen P, Kadzielski J, et al. Locking compression plates for osteoporotic nonunions of the diaphyseal humerus. *Clin Orthop Relat Res.* 2004;425:50–54.
- Kubiak EN, Fulkerson E, Strauss E, et al. The evolution of locked plates. *J Bone Joint Surg Am.* 2006;88(Suppl 4):189–200.
- Perren SM. Evolution of the internal fixation of long bone fractures. The scientific basis of biological internal fixation: choosing a new balance between stability and biology. *J Bone Joint Surg Br.* 2002;84:1093–1110.
- Egol KA, Kubiak EN, Fulkerson E, et al. Biomechanics of locked plates and screws. *J Orthop Trauma.* 2004;18:488–493.
- Claes LE, Heigele CA, Neidlinger-Wilke C, et al. Effects of mechanical factors on the fracture healing process. *Clin Orthop Relat Res.* 1998;355(Suppl):S132–S147.
- Duda GN, Söllmann M, Sporrer S, et al. Interfragmentary motion in tibial osteotomies stabilized with ring fixators. *Clin Orthop Relat Res.* 2002;396:163–172.
- Goodship AE, Kenwright J. The influence of induced micromovement upon the healing of experimental tibial fractures. *J Bone Joint Surg Br.* 1985;67:650–655.
- Augat P, Penzkofer R, Nolte A, et al. Interfragmentary movement in diaphyseal tibia fractures fixed with locked intramedullary nails. *J Orthop Trauma.* 2008;22:30–36.

11. Hente R, Fuchtmeier B, Schlegel U, et al. The influence of cyclic compression and distraction on the healing of experimental tibial fractures. *J Orthop Res*. 2004;22:709–715.
12. Kershaw CJ, Cunningham JL, Kenwright J. Tibial external fixation, weight bearing, and fracture movement. *Clin Orthop Relat Res*. 1993;293:28–36.
13. Egger EL, Gottsauner-Wolf F, Palmer J, et al. Effects of axial dynamization on bone healing. *J Trauma*. 1993;34:185–192.
14. Fitzpatrick DC, Doornink J, Madey SM, et al. Relative stability of conventional and locked plating fixation in a model of the osteoporotic femoral diaphysis. *Clin Biomech (Bristol, Avon)*. 2009;24:203–209.
15. Uthoff HK, Poitras P, Backman DS. Internal plate fixation of fractures: short history and recent developments. *J Orthop Sci*. 2006;11:118–126.
16. Henderson C, Bottlang M, Marsh JL, et al. Does locked plating of periprosthetic supracondylar femur fractures promote bone healing by callus formation? Two cases with opposite outcomes. *Iowa Orthop J*. 2009;28:73–75.
17. Button G, Wolinsky P, Hak D. Failure of less invasive stabilization system plates in the distal femur: a report of four cases. *J Orthop Trauma*. 2004;18:565–570.
18. Sommer C, Gautier E, Muller M, et al. First clinical results of the Locking Compression Plate (LCP). *Injury*. 2003;34(Suppl 2):B43–B54.
19. Stoffel K, Dieter U, Stachowiak G, et al. Biomechanical testing of the LCP—how can stability in locked internal fixators be controlled? *Injury*. 2003;34(Suppl 2):B11–B19.
20. Field JR, Tornkvist H, Hearn TC, et al. The influence of screw omission on construction stiffness and bone surface strain in the application of bone plates to cadaveric bone. *Injury*. 1999;30:591–598.
21. Stoffel K, Lorenz KU, Kuster MS. Biomechanical considerations in plate osteosynthesis: the effect of plate-to-bone compression with and without angular screw stability. *J Orthop Trauma*. 2007;21:362–368.
22. Tandon SC, Thomas PB. Standardisation of radiographic views of the fractured tibia. *J R Coll Surg Edinb*. 1999;44:241–243.
23. Eastaugh-Waring SJ, Joslin CC, Cunningham JL. Quantification of fracture healing from radiographs using the maximum callus index. *Clin Orthop Relat Res*. 2009;467:1986–1991.
24. Marsh JL, Slong TF, Agel J, et al. Fracture and dislocation classification compendium – 2007: Orthopaedic Trauma Association classification, database and outcomes committee. *J Orthop Trauma*. 2007;21:S1–S133.
25. Malizos KN, Papachristos AA, Protopoulos VC, et al. Transosseous application of low-intensity ultrasound for the enhancement and monitoring of fracture healing process in a sheep osteotomy model. *Bone*. 2006;38:530–539.
26. Tiedeman JJ, Lippiello L, Connolly JF, et al. Quantitative roentgenographic densitometry for assessing fracture healing. *Clin Orthop Relat Res*. 1990;253:279–286.
27. Lujan TJ, Henderson CE, O'Donovan M, et al. ASME Summer Bioengineering Conference; Lake Tahoe, CA; June 17–21, 2009. Abstract #206826.
28. Anderson DD, Mosqueda T, Thomas T, et al. Quantifying tibial plafond fracture severity: absorbed energy and fragment displacement agree with clinical rank ordering. *J Orthop Res*. 2008;26:1046–1052.
29. Holm S. A simple sequentially rejective multiple test procedure. *Scan J Stat*. 1979;6:65–70.
30. Weight M, Collinge C. Early results of the less invasive stabilization system for mechanically unstable fractures of the distal femur (AO/OTA types A2, A3, C2, and C3). *J Orthop Trauma*. 2004;18:503–508.
31. Syed AA, Agarwal M, Giannoudis PV, et al. Distal femoral fractures: long-term outcome following stabilisation with the LISS. *Injury*. 2004;35:599–607.
32. Wong MK, Leung F, Chow SP. Treatment of distal femoral fractures in the elderly using a less-invasive plating technique. *Int Orthop*. 2005;29:117–120.
33. Fankhauser F, Gruber G, Schippinger G, et al. Minimal-invasive treatment of distal femoral fractures with the LISS (Less Invasive Stabilization System): a prospective study of 30 fractures with a follow up of 20 months. *Acta Orthop Scand*. 2004;75:56–60.
34. Ricci WM, Loftus T, Cox C, et al. Locked plates combined with minimally invasive insertion technique for the treatment of periprosthetic supracondylar femur fractures above a total knee arthroplasty. *J Orthop Trauma*. 2006;20:190–196.
35. Schutz M, Muller M, Krettek C, et al. Minimally invasive fracture stabilization of distal femoral fractures with the LISS: a prospective multicenter study. Results of a clinical study with special emphasis on difficult cases. *Injury*. 2001;32(Suppl 3):SC48–SC54.
36. Herrera DA, Kregor PJ, Cole PA, et al. Treatment of acute distal femur fractures above a total knee arthroplasty: systematic review of 415 cases (1981–2006). *Acta Orthop*. 2008;79:22–27.
37. Schutz M, Muller M, Regazzoni P, et al. Use of the less invasive stabilization system (LISS) in patients with distal femoral (AO33) fractures: a prospective multicenter study. *Arch Orthop Trauma Surg*. 2005;125:102–108.
38. Marsh D. Concepts of fracture union, delayed union, and nonunion. *Clin Orthop Relat Res*. 1998;355(Suppl):S22–S30.
39. Markel MD, Chao EY. Noninvasive monitoring techniques for quantitative description of callus mineral content and mechanical properties. *Clin Orthop Relat Res*. 1993;293:37–45.
40. McKibbin B. The biology of fracture healing in long bones. *J Bone Joint Surg Br*. 1978;60:150–162.
41. Hammer RR, Hammerby S, Lindholm B. Accuracy of radiologic assessment of tibial shaft fracture union in humans. *Clin Orthop Relat Res*. 1985;199:233–238.
42. McClelland D, Thomas PB, Bancroft G, et al. Fracture healing assessment comparing stiffness measurements using radiographs. *Clin Orthop Relat Res*. 2007;457:214–219.
43. Oni OO, Dunning J, Mobbs RJ, et al. Clinical factors and the size of the external callus in tibial shaft fractures. *Clin Orthop Relat Res*. 1991;273:278–283.
44. Augat P, Merk J, Genant HK, et al. Quantitative assessment of experimental fracture repair by peripheral computed tomography. *Calcif Tissue Int*. 1997;60:194–199.
45. Gerstenfeld LC, Alkhiary YM, Krall EA, et al. Three-dimensional reconstruction of fracture callus morphogenesis. *J Histochem Cytochem*. 2006;54:1215–1228.
46. Whelan DB, Bhandari M, McKee MD, et al. Interobserver and intraobserver variation in the assessment of the healing of tibial fractures after intramedullary fixation. *J Bone Joint Surg Br*. 2002;84:15–18.
47. Bhandari M, Guyatt GH, Swiontkowski MF, et al. A lack of consensus in the assessment of fracture healing among orthopaedic surgeons. *J Orthop Trauma*. 2002;16:562–566.